https://doi.org/10.5194/egusphere-2023-431
Preprint. Discussion started: 28 March 2023
© Author(s) 2023. CC BY 4.0 License.

Technical Note: On HALOE stratospheric water vapor variations and trends at Boulder, Colorado

by

Ellis Remsberg
Science Directorate
21 Langley Blvd., Mail Stop 401B
NASA Langley Research Center
Hampton, Virginia USA, 23681
(email: Ellis.E.Remsberg@nasa.gov)

Abstract. This study compares time series of stratospheric water vapor (SWV) data at 30 hPa from 1993 to 2005, based on sets of Halogen Occultation Experiment (HALOE) profiles above the Boulder, CO (40°N, 255°E) region and on local frost-point hygrometer (FPH) measurements. Their differing trends herein agree with previously published findings. The FPH trends are presumed to be accurate within their uncertainties, and there are no known measurement biases affecting the HALOE trends. However, the seasonal sampling from HALOE is deficient at 40°N from 2001 to 2005, especially during late winter and springtime. HALOE time series at 20 hPa clearly show a springtime maximum in SWV at 40°N. The retrievals of HALOE SWV have significant corrections for interfering aerosol extinction following the eruption of Pinatubo, but there is no evidence that those corrections cause incorrect SWV trends after 1992. Accordingly, this study finds that the SWV trends from HALOE and FPH agree within their uncertainties for the more limited time span of 1993 to 2002. Northern hemisphere time series and daily plots of SWV from the Limb Infrared Monitor of the Stratosphere (LIMS) experiment indicate that there is transport of filaments of high SWV from polar to middle latitudes during dynamically active, winter and springtime periods. Although FPH measurements sense SWV variations at all scales, the HALOE time series do not resolve small-scale structure because its time series data are based on an average of four or more occultations within a finite latitude/longitude sector. It is concluded that the variations and trends of HALOE SWV are accurate for 1993 to 2002 at 40°N and in accord with the spatial scales of its measurements and its sampling frequency over time.

https://doi.org/10.5194/egusphere-2023-431
Preprint. Discussion started: 28 March 2023
© Author(s) 2023. CC BY 4.0 License.

1. Background and Objective

There have been numerous studies of long-term changes of stratospheric water vapor (SWV) mixing ratios (e.g., Konopka, et al., 2022; Hegglin et al., 2014; Hurst et al., 2011). SWV trends in the lowermost stratosphere are affected mainly by non-zonal variations of the cold-point temperature (CPT) at the tropical tropopause, followed by transport of the associated relatively dry, entry-level air. Hegglin et al. (2014) also report on the roles of the oxidation of methane to water vapor in the middle and upper stratosphere and of changes in the Brewer/Dobson circulation (BDC) on water vapor trends throughout the stratosphere. One remaining puzzle is that the SWV trends from frost-point hygrometer (FPH) measurements above Boulder, CO, are more positive (or less negative) than zonal average and Boulder region analyses of SWV from the Halogen Occultation Experiment (HALOE), and those differences increase with altitude (Scherer et al., 2008). Lossow et al. (2018) cautioned that the trends over Boulder may not be representative of zonal-mean values, and Konopka et al. (2022) found from reanalysis data that there is a moistening above the Boulder region during late boreal winter and spring.

The present study reconsiders in Section 2 the SWV trends and variations at 30 hPa from HALOE measurements near Boulder for 1993 through 2005 and compares them in Section 3 with those from the Boulder FPH measurements that are assumed to be accurate. Section 4 considers whether there is any bias for the HALOE SWV trends and whether there is evidence for a springtime moistening at 40°N. Section 5 shows a time series of northern hemisphere SWV near 30 hPa from the Nimbus 7 Limb Infrared Monitor of the Stratosphere (LIMS) dataset of 1978-1979, as a diagnostic for a source of elevated SWV during springtime. Daily plots of geopotential height (GPH) and SWV show the effects of meridional transport SWV during a dynamically active period of February 1979. There are also instances of elevated SWV in HALOE SWV time series of subpolar latitudes. Section 6 concludes that the HALOE SWV variations and trends at 40°N are understandable and agree with those from FPH, given the spatial scales of their measurements and the reduction in sampling by HALOE after 2001.

https://doi.org/10.5194/egusphere-2023-431
Preprint. Discussion started: 28 March 2023
© Author(s) 2023. CC BY 4.0 License.

2. Time series analyses of HALOE SWV near Boulder

SWV time series from the HALOE dataset are analyzed by multiple linear regression (MLR) techniques in the manner of Remsberg (2008) and Remsberg et al. (2018a). Figure 1 shows HALOE time series data from late 1991 through 2005 for the Boulder sector plus an MLR model fit to them, after correction for autoregressive effects having a lag-1 coefficient (AR1) of 0.35. Although HALOE began operations in October 1991, its SWV profiles are degraded in the lower stratosphere in 1991 through mid-1992 because of solar tracking anomalies in the presence of the very large extinction effects from Pinatubo aerosols. The MLR modeling of the data in Fig. 1 extends from January 1993 onward. Yet, there are indications that HALOE SWV is larger for SR than for SS from 2002 through 2005. Those apparent differences are because HALOE was turned on later following a UARS yaw maneuver and turned off a bit earlier prior to the next yaw event, to conserve power on the UARS spacecraft those years. That change in operating procedure meant that there were few to no HALOE SR measurements near 40°N during late winter and springtime after 2001.

The Boulder region HALOE SWV points of Fig. 1 are for 30 hPa and are based on averages of profiles within the latitude range of 40±4°N and the longitude range of 255±35°E, since HALOE seldom measured profiles at the exact location of Boulder. A rather narrow latitude range was chosen for this study because there is a significant latitudinal gradient in SWV near 40°N in both fall and springtime. The finite longitude range of ±35° attains four or more profiles from the SR or SS orbital crossings near Boulder, most times, and it is sufficient for resolving any zonal wave-1 and wave-2 features in the SWV field. The MLR model fit to the data of January 1993 through 2005 includes constant and linear trend terms plus periodic annual (AO), semiannual (SAO) and QBO-like terms, where the QBO-like term is approximated as a 28-mo cycle. The model also contains proxy terms for El Nino/Southern Oscillation (ENSO) and solar cycle flux forcings. Significant terms are SAO, QBO-like, and ENSO proxy; the latter two terms account for differences from the fit of the HALOE data in Fig. 1 versus that from a simple seasonal fitting, as shown in SPARC (2000, Chapter 3). The straight line in Fig. 1 represents the sum of the constant term (4.84 ppmv) and linear trend term of -4.4±0.7(2σ) %/decade with a confidence interval (CI) of 95%. The SWV trend from Fig. 1 agrees closely with the zonal mean trend at

https://doi.org/10.5194/egusphere-2023-431
Preprint. Discussion started: 28 March 2023
© Author(s) 2023. CC BY 4.0 License.

31.6 hPa from HALOE for the latitude range of 35°N to 45°N (Davis et al., 2016). Figure 2 is the residual (data minus MLR model curve) for the fit in Fig. 1, and its variations about the mean are of order ±0.3 ppmv.

Occultation time series points for Fig. 1 are not spaced regularly, so the derived MLR terms are non-orthogonal. However, the MLR term coefficients are reasonably accurate, if the seasonal sampling is good. Otherwise, the analyzed errors for each term become larger. The negative SWV trend is clearer from 2002 onward. Scherer et al. (2008), Hegglin et al. (2014), and Konopka et al. (2022) noted that there was a clear decrease in SWV in the tropical lower stratosphere in early 2001. They reported on a delay in the decrease of SWV at 40°N because of the slow ascent of the dry tropical air plus the subsequent meridional transport and mixing of that air to middle latitudes. As also noted by Scherer et al. (2008), it is perhaps more appropriate to apply two, piecewise linear trend terms for the MLR modeling of the HALOE SWV data in Fig. 1, where there is a break point in 2002. Instead, Figure 3 shows a separate trend analysis of HALOE SWV for the Boulder sector, but for 1993 to 2002; its average SWV value is 4.62 ppmv and its trend is no longer negative but positive or +4.4±0.8(2σ) %/decade.

3. Time series of FPH measurements of SWV

Figure 4 is the SWV time series at 30 hPa from the FPH data at Boulder and for 1993-2005 for comparison with Fig. 1. Individual FPH profiles were interpolated vertically to obtain SWV values at the 30-hPa level, and the FPH time series points are also spaced irregularly. SAO, ENSO, and Linear terms from the MLR model of Fig. 4 have a significance (CI) of better than 90%. The constant term is 4.70 ppmv, which is a bit less than that from the HALOE series (4.83 ppmv) but within the estimated systematic uncertainties for both measurements. The FPH trend for 1993-2005 is positive or +3.4±1.5 (2σ) %/decade, as compared to the negative trend from HALOE (-4.4±0.7 (2σ) %/decade). Figure 5 shows the residual (FPH minus MLR) for the time series data of Fig. 4, and the FPH points exhibit more scatter compared with the HALOE residual in Fig. 2. The larger scatter agrees reasonably with the upper limit, FPH uncertainty estimate of ±10% or about ±0.5 ppmv (SPARC, 2000). Accordingly, it is more difficult for the MLR

https://doi.org/10.5194/egusphere-2023-431
Preprint. Discussion started: 28 March 2023
© Author(s) 2023. CC BY 4.0 License.

modeling to resolve the periodic (SAO, AO, and QBO) variations from FPH data, while fitting a trend term.

All data points of the FPH record are assumed to be valid and accurate to 10%, based on the extensive studies reported in Hurst et al. (2023). Yet, Fig. 4 shows that FPH has high SWV values of 5.8 ppmv on 22 May and 5.5 ppmv on 26 June 1996, possibly due to elevated SWV in filaments of polar vortex air that were transported to and remained isolated above the location of Boulder for days to weeks (e.g., Manney et al. (2022)). A search of individual profiles from HALOE reveals SWV values of order 6.5 ppmv at 60°N, 270°E in mid-March 1996. Temperature at that higher latitude location is only 200 K and methane is only 0.4 ppmv, both of which are characteristic of winter vortex air. HALOE also found a small region of high SWV (~5.8 ppmv) and low methane in several soundings near 44°N, 170°E on 12 May 1996. In another instance, FPH has a value of 5.9 ppmv on 12 April 2000. HALOE SWV approached 7.0 ppmv near 60°N, 270°E about a month earlier on 18 March 2000; there are also several values greater than 5.0 ppmv at 40°N on 20 April 2000. Still, each individual HALOE profile gives SWV values that are an average across its tangent view path of order 300 km and with a vertical resolution of no better than two kilometers. The HALOE time series points are also based on sector averages of four or more profiles, so they do not resolve SWV variations at small to intermediate scales. Conversely, the local FPH measurements are sensitive to SWV variations across all spatial scales.

There is also a change in trend around 2002 in the FPH data of Fig. 4, although it is not so apparent because of the rather large scatter for the points of its data series. Figure 6 shows the MLR analysis of FPH data for 1993 to 2002, which yields an average SWV of 4.64 ppmv that agrees with the average value from HALOE in Fig. 3 (4.62 ppmv). The FPH trend for 1993 to 2002 is +5.8±1.2 %/decade and agrees with that from HALOE (+4.4±0.8 %/decade), at least within their combined uncertainties.

4. Uncertainties for the HALOE SWV trends

https://doi.org/10.5194/egusphere-2023-431
Preprint. Discussion started: 28 March 2023
© Author(s) 2023. CC BY 4.0 License.

As noted in the previous section, the SWV trend at 30 hPa from FPH is more positive (+5.8 %/decade) than that from HALOE (+4.4 %/decade) from 1993 to 2002, or prior to the episodic decrease of SWV from 2001. Gordley et al. (2009) reported that there are no indications of an instrument bias for the HALOE SWV trends. There are significant aerosol corrections for the retrieval of HALOE SWV in the lower stratosphere, especially following the Pinatubo eruption. Harries et al. (1996) estimated that a given HALOE SWV profile is uncertain by 6% to 8% at 10 hPa and 40 hPa, respectively, due to aerosols. Yet, the corrections are relatively accurate with time because each individual SWV profile makes use of a corresponding estimate of aerosol extinction from another HALOE channel of the same occultation sounding. Aerosol extinction profiles are determined for wavelengths of the HALOE gas filter correlation channels of HF, HCl, CH_4, and NO (Hervig et al., 1995). Then, corrections for the HALOE radiometer channels (H_2O, NO_2, and O_3) are a modeled extrapolation in wavelength from the NO channel aerosol profile at 5.26 micrometers. Example comparisons of retrieved HALOE SWV versus correlative measurements indicate that the modeled corrections are qualitatively accurate, even in 1992. Nevertheless, the model for aerosol absorption versus wavelength assumes a size distribution shape and an aqueous sulfuric acid composition (i.e., refractive index) that is constant with altitude and over time (Hervig et al., 1996). Effectively, the aerosol correction represents a change in aerosol number density only. That model may not be very accurate for the Pinatubo layer, as it decays over time. Thus, there may be a residual, time dependent bias for the HALOE SWV due to the aerosol correction model.

As a check on that possibility, Figure 7 shows the corresponding fit of the HALOE SWV time series from 1993 to 2002 at 40°N and 20 hPa, or just above the top of volcanic aerosol layer. SWV has a positive vertical mixing ratio gradient with altitude, due to the oxidation of methane to SWV in the middle stratosphere, and average SWV at 20 hPa is 4.74 ppmv or higher than that at 30 hPa (4.62 ppmv). A combined AO/SAO maximum shows clearly in Fig. 7, where the AO amplitude is twice that of the SAO and the AO and SAO phase maxima are on 19 February and 9 April, respectively. Those cycles confirm the late winter/early spring moistening found in reanalysis data by Konopka et al. (2022).

https://doi.org/10.5194/egusphere-2023-431
Preprint. Discussion started: 28 March 2023
© Author(s) 2023. CC BY 4.0 License.

The HALOE SWV trend at 20 hPa is +6.6±0.9 (2σ) %/decade, which is a bit higher than that from FPH (+5.8±1.2 %/decade) at 30 hPa but within uncertainties. (There are too few FPH data at 20 hPa for a direct trend comparison with HALOE.) On the other hand, the HALOE trend at 20 hPa is significantly more positive than the HALOE trend at 30 hPa (+4.4±0.8 %/decade), although a positive difference is expected because of the effects of the oxidation of methane to water vapor. Remsberg (2015, Table 1) reported significant positive trends of order 10%/decade in the tropical middle stratosphere for HALOE methane, a small fraction (certainly less than half) of which has undergone oxidization to SWV and a transport to 40°N and 20 hPa. Thus, the increase of 2.2%/decade in the HALOE SWV trend from 30 to 20 hPa may be accounted for by those processes alone; the aerosol corrections may be sufficiently accurate after 1992.

5. Source for the springtime moistening at 40°N

Hegglin et al. (2014) and Remsberg (2015) showed that both methane and water vapor from limb-viewing satellite datasets (SPARC, 2017) are good indicators of seasonal variations of the BDC in the stratosphere. They reported on a hemispheric asymmetry for the net circulation, where the BDC in the northern hemisphere (NH) is stronger and its methane and relative SWV trends are more positive than in the southern hemisphere. The strength of the NH BDC is enhanced in winter, primarily due to effects of forcings from planetary waves. The chemical conversion of methane to water vapor in the middle and upper stratosphere is followed by descent of that relatively moist air to the lower stratosphere in the region of the polar vortex.

Seasonal SWV data from the LIMS experiment illustrate the above process for 1978-1979. Figure 8 (from Remsberg et al., 2018b, their Fig. 14) displays this seasonal increase in a time series of SWV for the NH on the 550 K potential temperature surface (near 30 hPa) in terms of its area diagnostic versus equivalent latitude, which is a vortex-centered display of SWV along potential vorticity contours. Fig. 8 indicates that enhanced values of water vapor descended to this surface in the vortex region by early January and continued through March. Specifically, there was an expansion of the average SWV value of 5.2 ppmv to the equivalent latitude of 40°N during mid-February and from mid-March onward, as the high latitude air mixed with lower latitude air. Note that the 550 K surface is well above the tropical tropopause, minimizing

© Author(s) 2023. CC BY 4.0 License.

effects due to any meridional exchanges of water vapor within the lowermost stratosphere. Similar analyses of seasonal changes of ozone also show that there is further descent to lower potential temperature levels during springtime and a similar transport and mixing of polar air to lower latitudes at those levels (Curbelo et al., 2021).

Polar plots of LIMS Version 6 (V6) geopotential height (GPH) and SWV for 17 February 1979 are in Figures 9 and 10. They indicate the effects of meridional transport of polar air to middle latitudes, in response to a high latitude, zonal wave-2 event. Fig. 9 shows high GPH (and anticyclonic circulation) in the Aleutian and eastern Atlantic sectors and low GPH in the polar vortex (cyclonic) that extends southward across North America. The associated higher values of SWV in Fig. 10, though somewhat noisy, are characteristic of vortex air that also underwent a southward transport. The vortex (region of highest SWV) is elongated and extends equatorward around 90°E and 270°E. There is also a filament of high SWV (>5.5 ppmv) at the latitude of Boulder and across adjacent longitudes. The seasonal time series display of NH SWV in Fig. 8 shows that this is when the 5.2 ppmv contour extends to near 40°N equivalent latitude.

Figure 8 also indicates that there was an initial descent of polar air with higher values of SWV to near the 31.6 hPa surface around 10 January. Then there was a more general expansion of SWV by the end of January to the equivalent latitude of 40°N (follow the 4.8 ppmv contour in Fig. 8). Similar instances of meridional transport and mixing to North American middle latitudes are a likely cause of the sporadic appearance of similar high SWV values during the winter and early spring seasons in the FPH measurements of Fig. 4 and in the recent reanalysis studies of Konopka et al. (2022) and of Wargan et al. (2023). However, the HALOE time series points in Figs. 1 and 3 do not resolve such features because they are based on averages of four or more profiles from within the rather large sector around Boulder.

HALOE SWV time series were also analyzed for occurrences of higher SWV in three separate longitude sectors (North America, 255±35°E; Aleutian, 180±35°E; and European, 35±35°E) from 1993 to 2002. There are several instances at 40°N in the Boulder sector (Fig. 3), but none

© Author(s) 2023. CC BY 4.0 License.

in the Aleutian or European sectors (not shown). However, Figure 11 shows that there are several positive anomalies in the European sector at the higher latitude zone of 53±7°N, while there are none in the Boulder or Aleutian sectors (not shown). Average SWV from Fig. 11 is 5.14 ppmv, and SWV approaches 6.0 ppmv in four instances (on 22 April 1994, 14 April 1996, 7 March 2000, and 14-19 February 2001). All four instances are accompanied by low values of methane, which is also a tracer of the transport of polar air to lower latitudes. The instances in 2000 and 2001 also occurred, when temperatures in the upper stratosphere were of order 270 K or like that for a sudden stratospheric warming (SSW) event. There was a rather extended area of higher SWV over Europe at those times, not merely a filament of vortex air.

6. Summary and Conclusions

Analyses of time series of HALOE and FPH SWV were conducted at 30 hPa for the Boulder region. Sampling frequencies for both time series are only of the order of a week to a month or more. The SWV trend in the Boulder region is positive from the FPH and negative from the HALOE data from 1993 to 2005. It is assumed that the time series of FPH SWV measurements are accurate, at least within their uncertainties of ±10%; the foregoing HALOE/FPH trend differences appear significant. However, there are rather large gaps at 40°N during late winter and spring in the HALOE time series after 2001, due to the limited power that was available for HALOE operations. This makes it is more difficult to resolve the seasonal terms and the trend term from the HALOE time series after 2001.

The HALOE SWV trend goes from positive to negative around 2002, and that change is a delayed effect following the sharp decrease in tropical, lower stratospheric SWV that occurred early in 2001. The FPH time series has a trend that is less positive after 2001, too, although that change is not so obvious because of the larger scatter for its points. It is more appropriate to fit two, piecewise linear trends to both the HALOE and FPH time series with a break point in 2002. There are no known measurement biases that are affecting the HALOE trends, although the retrievals of HALOE SWV do have significant corrections for interfering aerosol extinction following the eruption of Pinatubo. However, there is no clear evidence that those corrections

https://doi.org/10.5194/egusphere-2023-431
Preprint. Discussion started: 28 March 2023
© Author(s) 2023. CC BY 4.0 License.

are affecting the SWV trends after 1992. Thus, it is concluded that the analyzed HALOE trend at 30 hPa (+4.4±0.8 %/decade) agrees with that from FPH (+5.8±1.2 %/decade) for 1993 to 2002 within their combined uncertainties.

The HALOE SWV time series at 20 hPa clearly shows a springtime maximum. Northern hemisphere SWV time series from the Limb Infrared Monitor of the Stratosphere (LIMS) experiment indicate a transport of SWV from polar to middle latitudes during late winter and springtime. Daily surface maps of LIMS SWV reveal instances of filamentary structure at the latitude of 40°N during and following dynamically active periods. Surface maps of GPH verify that there was meridional transport of high SWV from the polar vortex to the latitude of 40°N at those times. Whereas FPH measurements sense SWV variations at all scales, the HALOE time series of the present study do not resolve intermediate to smaller scale structure because its data points are based on an average of four or more occultation profiles within a finite latitude/longitude sector centered on Boulder. It is concluded that the variations and trends of HALOE SWV are accurate at 40°N for 1993 to 2002 and in accord with the spatial scales of its measurements and its sampling frequencies.

Data Availability

The LIMS V6 Level 3 product and the HALOE V19 profiles are at the NASA EARTHDATA site of EOSDIS and its Website as: https://disc.gsfc.nasa.gov/datacollection/LIMSN7L3_006.html, and as https://disc.gsfc.nasa.gov/datacollection/UARHA2FN_019.html, respectively.

Frost point hygrometer (Lev) data were downloaded from the NOAA website: https://gml.noaa.gov/aftp/data/ozwv/WaterVapor/Boulder_New/.

Competing interests: The author declares no competing interests.

https://doi.org/10.5194/egusphere-2023-431
Preprint. Discussion started: 28 March 2023
© Author(s) 2023. CC BY 4.0 License.

Acknowledgements. Author EER thanks V. Lynn Harvey for generating the plot in Figure 8 that appeared originally in Remsberg et al. (2018b). EER also appreciates comments by Mark Hervig about the manuscript. EER carried out this work while serving as a Distinguished Research Associate of the Science Directorate at NASA Langley.

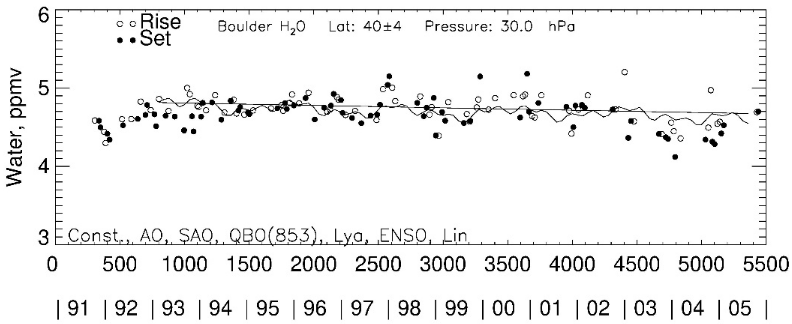

Figure 1—MLR fit to a HALOE SWV time series for the region above Boulder. The fit of all the MLR terms is shown as the oscillating curve; the linear trend term is the straight line. Time (in days) and year on abscissa begins on January 1, 1991.

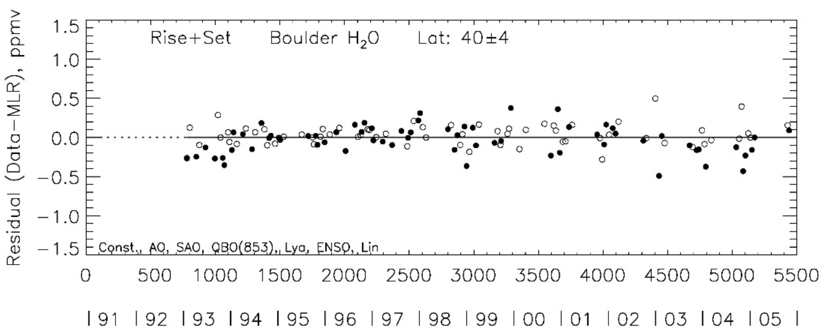

Figure 2—Residual from MLR model fit to HALOE time series data of Fig. 1.

https://doi.org/10.5194/egusphere-2023-431
Preprint. Discussion started: 28 March 2023
© Author(s) 2023. CC BY 4.0 License.

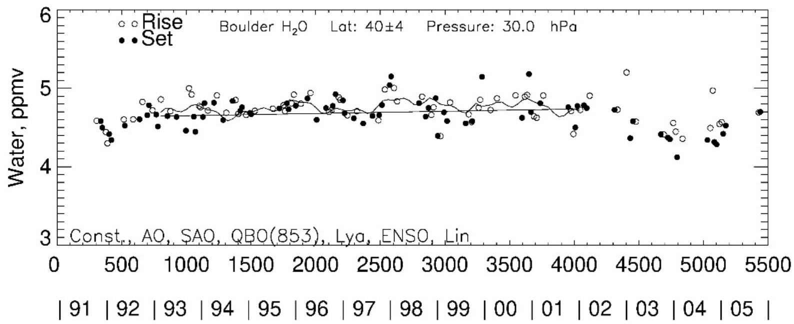

Figure 3—As in Fig. 1, but where the MLR fit for 40°N is from 1993 to 2002.

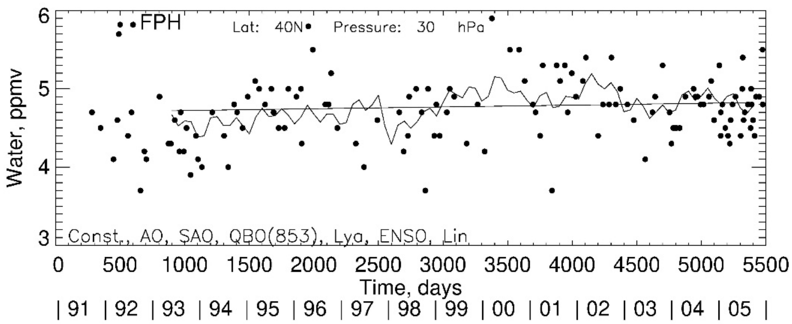

Figure 4—Time series of FPH data and MLR fit to them for comparison with Fig. 1.

https://doi.org/10.5194/egusphere-2023-431
Preprint. Discussion started: 28 March 2023
© Author(s) 2023. CC BY 4.0 License.

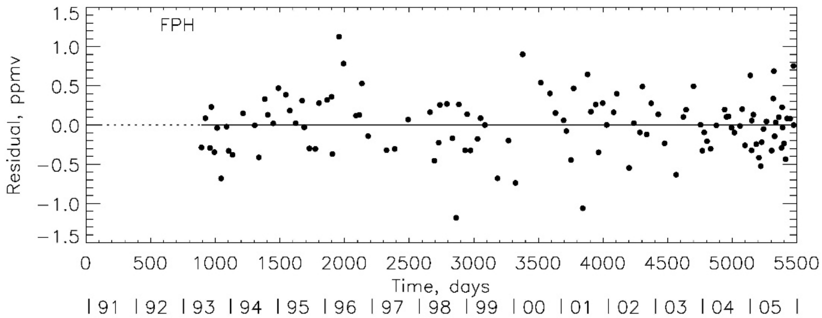

Figure 5—Time series residual for the MLR fit to the FPH data of Fig. 4.

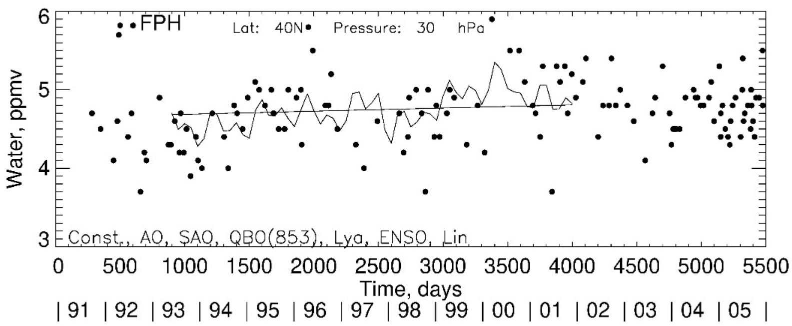

Figure 6—As in Fig. 4, but for 1993 to 2002.

https://doi.org/10.5194/egusphere-2023-431
Preprint. Discussion started: 28 March 2023
© Author(s) 2023. CC BY 4.0 License.

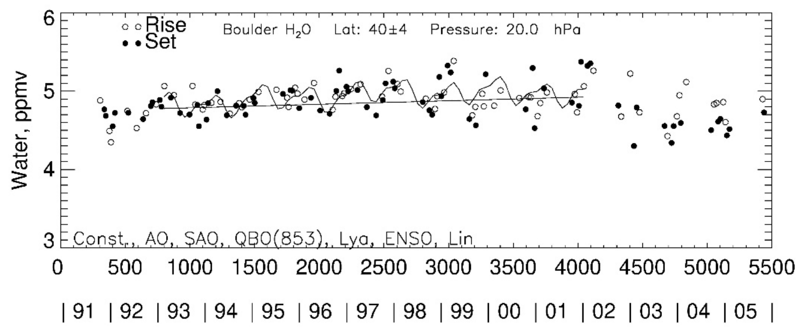

Figure 7—As in Fig. 3, but for HALOE data at 20 hPa.

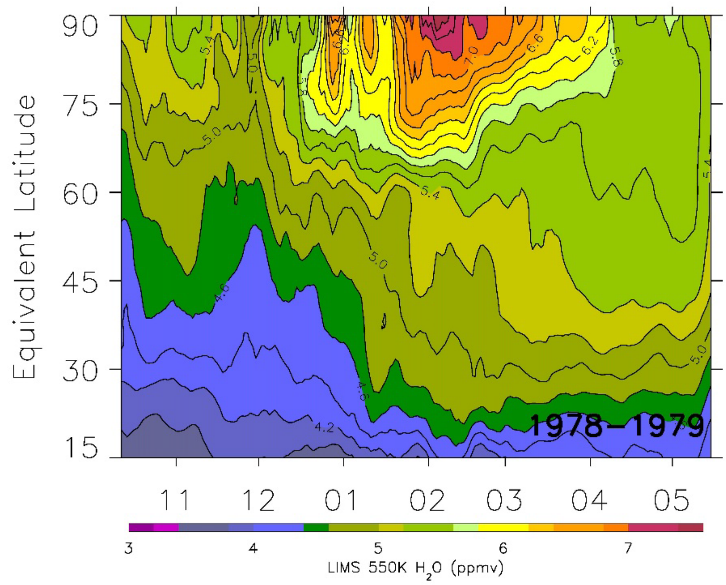

Figure 8—Time series of LIMS water vapor vs. equivalent latitude at 550 K and with smoothing over 7 days. Contour interval is 0.2 ppmv. Tic marks along the abscissa denote the middle of each month.

https://doi.org/10.5194/egusphere-2023-431
Preprint. Discussion started: 28 March 2023
© Author(s) 2023. CC BY 4.0 License.

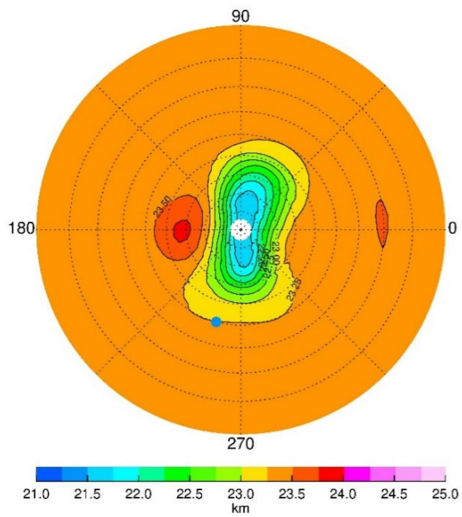

Figure 9—NH plot on the 31.6-hPa surface for 17 February 1979 of LIMS geopotential height (GPH). Contour increment for GPH is 0.25 gpkm, and dashed circles are at every 10° of latitude. Blue dot is location of Boulder, CO (40°N, 255°E).

https://doi.org/10.5194/egusphere-2023-431
Preprint. Discussion started: 28 March 2023
© Author(s) 2023. CC BY 4.0 License.

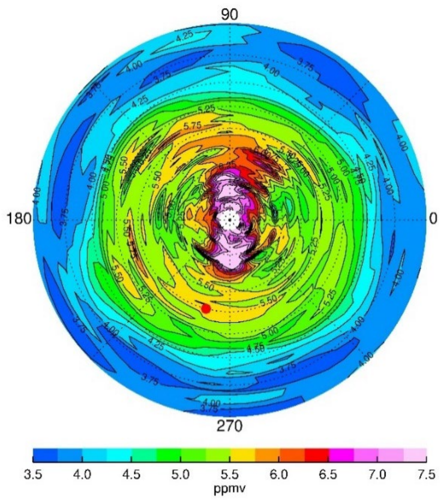

Figure 10—As in Fig. 9, but for LIMS SWV on 17 February. Contour interval (CI) is 0.25 ppmv. Red dot is location of Boulder.

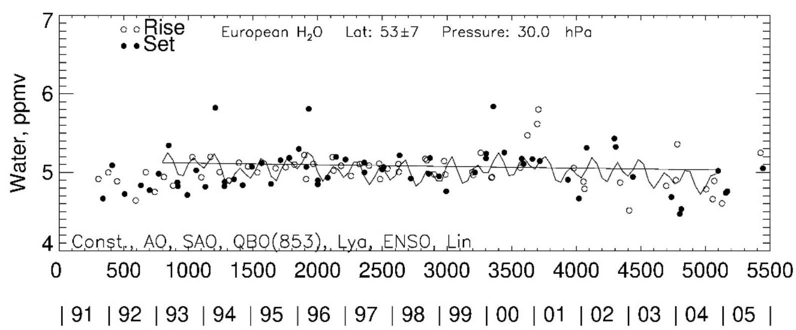

Figure 11—As in Fig. 1, but for a European sector, centered at 53°N, 35°E. Note that the HALOE SWV scale extends from 4 to 7 ppmv, unlike in Fig. 1.

© Author(s) 2023. CC BY 4.0 License.

References

Curbelo, J., Chen, G., & Mechoso, C. R.: Lagrangian analysis of the northern stratospheric polar vortex split in April 2020. Geophys. Res. Lett., 48, e2021GL093874. https://doi.org/10.1029/2021GL093874, 2021.

Davis, S. M., Rosenlof, K. H., Hassler, B., Hurst, D. F., Read, W. G., Vömel, H., Selkirk, H., Fujiwara, M., and Damadeo, R.: The stratospheric water and ozone satellite homogenized (SWOOSH) database: a long-term database for climate studies, Earth Syst. Sci. Data, 8, 461-490, www.earth-syst-sci-data.net/8/461/2016/doi:10.5194/essd-8-461-2016, 2016.

Gordley, L. L., Thompson, E., McHugh, M., Remsberg, E., Russell III, J., and Magill, B.: Accuracy of atmospheric trends inferred from the Halogen Occultation Experiment data, J. Appl. Remote Sensing, 3, https:// doi.org/10.1117/1.3131722, 2009.

Harries, J. E., Russell III, J. M., Tuck, A. F., Gordley, L. L., Purcell, P., Stone, K., Bevilacqua, R. M., Gunson, M., Nedoluha, G., and Traub, W. A.: Validation of measurements of water vapor from the Halogen Occultation Experiment (HALOE), J. Geophys. Res., 101, https://doi.org/10.1029/95JD02933C, 1996.

Hegglin, M. I., Plummer, D. A., Shepherd, T. G., Scinocca, J. F., Anderson, J., Froidevaux, L., Funke, B., Hurst, D., Rozanov, A., Urban, J., von Clarmann, T., Walker, K. A., Wang, H. J., Tegtmeier, S., and Weigel, K.: Vertical structure of stratospheric water vapour trends derived from merged satellite data, Nature Geoscience, 7(10), 768–776. https://doi.org/10.1038/NGEO2236, 2014.

Hervig, M. E., Russell III, J. M., Gordley, L. L., Park, J. H., Drayson, S. R., and Deshler, T.: Validation of aerosol measurements from the Halogen Occultation Experiment, J. Geophys. Res., 101, https://doi.org/10.1029/95JD02464, 1996.

https://doi.org/10.5194/egusphere-2023-431
Preprint. Discussion started: 28 March 2023
© Author(s) 2023. CC BY 4.0 License.

Hervig, M. E., Russell III, J. M., Gordley, L. L., Daniels, J., Drayson, S. R., Park, J. H.: Aerosol effects and corrections in the Halogen Occultation Experiment, J. Geophys. Res., 100, https://doi.org/10.1029/94JD02143, 1995.

Hurst, D. F., Fujiwara, M., and Oltmans, S.: Frost point hygrometers, in *Field Measurements for Passive Environmental Remote Sensing*, Elsevier, Inc., https://doi.org/10.1016/B978-0-12-823953-7.00015-0, 2023.

Hurst, D. F., Oltmans, S. J., Vömel, H., Rosenlof, K. H., Davis, S. M., Ray, E. A., Hall, E. G., and Jordan, A. F.: Stratospheric water vapor trends over Boulder, Colorado: Analysis of the 30 year Boulder record, J. Geophys. Res., 116, https://doi.org/10.1029/2010JD015065, 2011.

Konopka, P., Tao, M., Ploeger, F., Hurst, D. F., Santee, M. L., Wright, J. S., and Riese, M.: Stratospheric moistening after 2000, Geophysical Research Letters, 49, e2021GL097609. https://doi.org/10.1029/2021GL097609, 2022.

Lossow, S., Hurst, D. F., Rosenlof, K. H., Stiller, G. P., von Clarmann, T., Brinkop, S., Dameris, M., Jöckel, P., Kinnison, D. E., Plieninger, J., Plummer, D. A., Ploeger, F., Read, W. G., Remsberg, E. E., Russell III, J. M., and Tao, M.: Trend differences in lower stratospheric water vapour between Boulder and the zonal mean and their role in understanding fundamental observational discrepancies, Atmos. Chem. Phys., 18, 8331-8351, https://doi.org/10.5194/acp-18-8331-2018, 2018.

Manney, G. L., Millan, L. F., Santee, M. L., Wargan, K., Lambert, A., Neu, J. L., Werner, F., Lawrence, Z. D., Schwartz, M. J., Livesey, N. J., and Read, W. G.: Signatures of Anomalous Transport in the 2019/2020 Arctic Stratospheric Polar Vortex, J. Geophys. Res. Atmospheres, 127, e2022JD037407, https://doi.org/10.1029/2022JD037407, 2022.

Remsberg, E.: Methane as a diagnostic tracer of changes in the Brewer-Dobson circulation of the stratosphere, Atmos. Chem. Phys., 15, 3739-3754, https://doi.org/10.5194/acp-15-3739-2015, 2015.

Remsberg, E. E.: On the response of Halogen Occultation Experiment (HALOE) stratospheric ozone and temperature to the 11-yr solar cycle forcing, J. Geophys. Res.-Atmospheres, 113, https://doi.org/10.1029/2008JD010189, 2008.

Remsberg, E., Damadeo, R., Natarajan, M., and Bhatt, P.: Observed responses of mesospheric water vapor to solar cycle and dynamical forcings, J. Geophys. Res., 123, 3830-3843, https://doi.org/10.1002/2017JD028029, 2018a.

Remsberg, E., Natarajan, M., and Harvey, V. L: On the consistency of HNO3 and NO2 in the Aleutian High region from the Nimbus 7 LIMS Version 6 dataset, Atmos. Meas. Tech., 11, 3611-3626, https://doi.org/10.5194/amt-11-3611-2018, 2018b.

Scherer, M., Vömel, H., Fueglistaler, S., Oltmans, S.J., and Staehelin, J.: Trends and variability of midlatitude stratospheric water vapour deduced from the re-evaluated Boulder balloon series and HALOE, Atmos. Chem. Phys., 8, 1391–1402, www.atmos-chem-phys.net/8/1391/2008/, 2008.

SPARC *Report No. 2*: Upper Tropospheric and Stratospheric Water Vapour, Edited by D. Kley, J. M. Russell III, and C. Phillips, WCRP – 113, Geneva, https://www.sparc-climate.org/publications/sparc-reports/sparc-report-no-2/, 2000.

https://doi.org/10.5194/egusphere-2023-431
Preprint. Discussion started: 28 March 2023
© Author(s) 2023. CC BY 4.0 License.

SPARC *Report No. 8 of the SPARC Data Initiative*: Assessment of stratospheric trace gas and aerosol climatologies from satellite limb sounders, Prepared by the SPARC Data Initiative Team and edited by M. I. Hegglin and S. Tegtmeier, WCRP-5/2017, Geneva, https://doi.org/10.3929/ethz-a-010863911, 2017.

Wargan, K., Weir, B., Manney, G. L., Cohn, S. E., Knowland, K. E., Wales, P. A., and Livesey, N. J.: M2-SCREAM: A stratospheric composition reanalysis of Aura MLS data with MERRA-2 transport. Earth and Space Science, 10, e2022EA002632., https://doi.org/10.1029/2022EA002632, 2023.